

Characterization of a von Hippel Lindau Pathway Involved in Extracellular Matrix Remodeling, Cell Invasion, and Angiogenesis

Ghada Kurban,¹ Valérie Hudon,¹ Eric Duplan,¹ Michael Ohh,² and Arnim Pause¹

¹McGill Cancer Center and Department of Biochemistry, McGill University, Montreal, Quebec and ²Department of Laboratory Medicine and Pathobiology, Faculty of Medicine, University of Toronto, Toronto, Ontario, Canada

Abstract

Inactivation of the von Hippel-Lindau (VHL) tumor suppressor gene results in highly vascularized tumors, making the VHL tumor syndrome an ideal system to study the mechanisms of angiogenesis. VHL operates along two pathways with the first involving hypoxia-inducible factor- α degradation and down-regulation of its proangiogenic target genes vascular endothelial growth factor and platelet-derived growth factor- β , and the second pathway promoting extracellular matrix (ECM) assembly. Secretion of proangiogenic factors was shown to be a primary inducer of angiogenesis. Here, we show that loss of ECM assembly correlates with tumor angiogenesis in VHL disease. Upon inactivation of the VHL-ECM assembly pathway, we observe tumors that are highly vascularized, have a disrupted ECM, and show increased matrix metalloproteinase-2 activity. Loss of the VHL pathway leading to hypoxia-inducible factor- α degradation results in tumors with increased vascular endothelial growth factor levels but with surprisingly low microvessel density, a tightly assembled ECM and low invasive ability. We conclude that loss of ECM integrity could promote and maintain tumor angiogenesis by providing a route for blood vessels to infiltrate tumors. (Cancer Res 2006; 66(3): 1313-9)

Introduction

von Hippel-Lindau (VHL) disease is an autosomal dominant familial cancer syndrome caused by the germ line mutation of the VHL tumor suppressor gene (1). Loss of VHL function leads to the development of highly angiogenic tumors including renal cell carcinoma (RCC), hemangioblastomas of the central nervous system, and pheochromocytoma (2–4). These highly vascularized tumors make VHL disease an ideal model to study angiogenesis.

Angiogenesis, which involves the growth of new capillaries from preexisting microvessels, is critical for various physiologic and pathologic processes, particularly tumorigenesis and metastasis. Ever since tumor growth was proposed to be dependent on angiogenesis (5), numerous studies have shown that it is required for the growth and metastasis of solid tumors that are over a few cubic millimeters in size (6). The angiogenic response, also known as the “angiogenic switch,” is initiated when the balance between the positive and the negative regulators of angiogenesis is disrupted in favor of the proangiogenic factors (6, 7).

The role of VHL in the regulation of proangiogenic factors stems from its ability to down-regulate the alpha subunit of the hypoxia-inducible factor (HIF- α), which exists in at least three isoforms (HIF-1 α , HIF-2 α , and HIF-3 α ; ref. 8). The VHL protein is part of an E3 ubiquitin ligase complex which targets HIF- α for ubiquitylation and degradation by the 26S proteasome under normal oxygen levels (1, 9–15). Under hypoxic conditions or on loss of VHL function, HIF- α is stabilized, resulting in transcription and accumulation of various HIF target genes such as vascular endothelial growth factor (VEGF), platelet-derived growth factor- β , transforming growth factor- α , and glucose transporter 1 (GLUT-1; refs. 1, 8). It was recently shown that HIF-2 α is the isoform responsible for the induction of proangiogenic and growth factors (16).

In addition to HIF- α regulation, VHL also plays an important role in maintaining extracellular matrix (ECM) integrity (1, 17–19). VHL-negative cells lose the ability to assemble a fibronectin matrix whereas reintroduction of VHL restores assembly (17, 18). ECM assembly is an important regulatory element of blood vessel formation. Degradation of ECM by various proteases allows endothelial cell migration, leads to the release of ECM-sequestered angiogenic factors, and results in blood vessel infiltration (20, 21). VHL was reported to interact with a 200 kDa protein (9, 22) that was subsequently identified as fibronectin (17). This interaction is lost with all naturally occurring VHL mutants tested to date, stressing its importance in the VHL disease (1).

The significance of matrix disassembly in VHL disease is not well understood. However, it was reported that VHL neddylation is required for fibronectin matrix assembly and leads to suppression of tumorigenesis (23). Moreover, a recent study of VHL function in *Caenorhabditis elegans* confirmed that VHL operates along two independent pathways; one being dependent on HIF- α , and the other involving ECM regulation (24), suggesting evolutionary conservation of both pathways. Here, we used a cellular system in which the VHL-ECM assembly and VHL-HIF-2 α degradation pathways are uncoupled to study their contribution to invasion, tumorigenesis, and angiogenesis.

We show that VHL leads to the assembly of a fibronectin and collagen type IV network which correlates with suppression of invasiveness *in vitro* as well as angiogenesis and tumorigenesis *in vivo*. VEGF expression in VHL tumors is not sufficient to promote and maintain angiogenesis unless it is coupled with an aberrantly remodeled ECM matrix suitable for endothelial cell migration and blood vessel infiltration. We conclude that loss of the VHL-ECM assembly pathway is likely to promote angiogenesis activation which could lead to highly vascularized VHL tumors. These results might have implications for the induction of angiogenesis in other carcinomas.

Materials and Methods

Cells and cell culture. VHL-negative human renal carcinoma cell line 786-0, as well as stable transfectants of 786-0, including pRC-HAVHL clones

Note: G. Kurban and V. Hudon contributed equally to this work.

Requests for reprints: Arnim Pause, McGill Cancer Center and Department of Biochemistry, McGill University, 3655 Promenade Sir William Osler, Room 716, Montreal, Quebec, H3G 1Y6. Phone: 514-398-1521; Fax: 514-398-6769; E-mail: arnim.pause@mcgill.ca.

©2006 American Association for Cancer Research.
doi:10.1158/0008-5472.CAN-05-2560

WT8 and WT7, pRC vector alone clone pRC3, pRC-HAVHL mutant L188V, pRC-HAVHL mutant R64P, and pRC-HAVHL pools of WT8 clones transduced either with an empty retroviral vector (WTE) or a retrovirus expressing a mutant P531A HIF2 α (WTPA) were a kind gift from Dr. William G. Kaelin (Dana-Farber Cancer Institute and Brigham and Women's Hospital, Harvard Medical School, Boston, MA). These cell lines have been described previously (18, 25). All the cells were grown in DMEM (Invitrogen, Burlington, Ontario, Canada) supplemented with 10% fetal bovine serum (FBS; Sigma-Aldrich Canada Ltd., Oakville, Ontario, Canada), 0.5 mg/mL G-418 in addition to 1.5 μ g/mL of puromycin (in case of the retrovirally transduced cell lines) and maintained at 37°C in an atmosphere of 5% CO₂.

Antibodies. The primary antibodies used were mouse anti-human fibronectin (BD Biosciences Pharmingen, Mississauga, Ontario, Canada), mouse anti-human collagen type IV (Chemicon, Temecula, CA), rabbit anti-human collagen type IV (Abcam, Cambridge, MA), rabbit anti-GLUT-1 (Alpha Diagnostic, San Antonio, TX), rabbit anti-HIF-2 α (Novus, Littleton, CO), mouse anti-HA (12CA5; Roche, Laval, Quebec, Canada), rabbit anti-VEGF (Neomarkers, Labvision, Fremont, CA), and rat anti-mouse CD31 (BD Pharmingen). Mouse anti-MMP-2 was kindly provided by Dr. Rafael Friedman (Wayne State University, Detroit, MI). Secondary antibodies used were rhodamine-conjugated goat anti-mouse, FITC-conjugated goat anti-mouse, horseradish peroxidase-conjugated anti-mouse (Jackson ImmunoResearch Laboratories, Inc., West Grove, PA) as well as horseradish peroxidase-conjugated anti-rabbit (Amersham).

Immunofluorescence microscopy. Cells (5×10^5) were grown on coverslips in six-well plates for 6 days. They were then washed with PBS, fixed with 95% ethanol at -20°C, followed by incubation with an antifibronectin monoclonal antibody. They were then washed with PBS-0.1% Tween and incubated with the secondary rhodamine-conjugated goat anti-mouse antibody. The nuclei were finally stained with 4',6-diamidino-2-phenylindole hydrochloride (Sigma) and the cells were visualized using a Zeiss immunofluorescent microscope.

Nude mouse xenograft assays. To perform tumor inoculation, the different cell lines were harvested by trypsinization. Cell concentration and viability were determined by trypan blue staining, and 10^7 cells resuspended in sterile PBS were injected s.c. into both flanks of 6- to 8-week-old CD1 nude (*nu/nu*) mice (Charles River Laboratories, Wilmington, MA). Nine to 10 weeks after injection, the animals were sacrificed and the s.c. tumors were excised. Bidimensional measurements were done using calipers and tumor volumes were calculated using the following formula: volume = width² \times length / 2. The tumors were either embedded in optimal cutting temperature freezing medium (Tissue Tek, Sakura Finetek USA, Inc., Torrance, CA) and stored at -80°C, or they were fixed in 4% paraformaldehyde/PBS overnight and embedded into paraffin for immunohistochemical analysis.

Immunohistochemistry. Ten-micrometer frozen sections of tumors were fixed in ice-cold acetone and rinsed in PBS. After blocking in PBS-0.05% Tween containing 1% (w/v) bovine serum albumin (BSA), sections were incubated with mouse anti-human collagen type IV and mouse anti-human fibronectin. The sections were then washed in PBS-0.05% Tween and incubated with FITC-conjugated goat anti-mouse IgGs. Finally, the sections were stained with 4',6-diamidino-2-phenylindole and mounted using fluorescent mounting medium (DAKO Canada Inc., Mississauga, Ontario, Canada).

For visualization of blood vessels, frozen sections were incubated with an anti-CD31 antibody, followed by an incubation with goat anti-rat secondary antibody (Vector Laboratories, Inc., Burlingame, CA). The signal was enhanced using an ABC kit (Vector) and color was developed with the chromophore diaminobenzidine (Sigma). Sections were counterstained with Fast Red nuclear (Sigma). Microvessel density was carried out from three random fields (magnification, $\times 20$) and quantified using ImageJ software following CD31 staining.

VEGF staining was done on paraffin sections. Before immunostaining, antigen retrieval was done by incubating the sections with antigen unmasking solution (Vector), and endogenous peroxidase activity was inhibited with 1% hydrogen peroxide. The sections were then incubated overnight at 4°C with the primary antibody. Color development was achieved in the same manner as for the CD31 staining, and sections were finally counterstained with hematoxylin.

VEGF ELISA. The various cell lines were seeded in six-well plates (5×10^4 cells/well) and allowed to grow for 72 hours in normal growth medium. The conditioned medium was then removed, and VEGF levels were assayed by ELISA (R&D Systems, Minneapolis, MN) according to the manufacturer's protocol. For normalization, the VEGF protein level was divided by the total cellular protein concentration for each sample.

Western blots. For fibronectin and collagen IV expression levels, cells were grown in 10 cm plates and lysed using an EBC buffer [50 mmol/L Tris

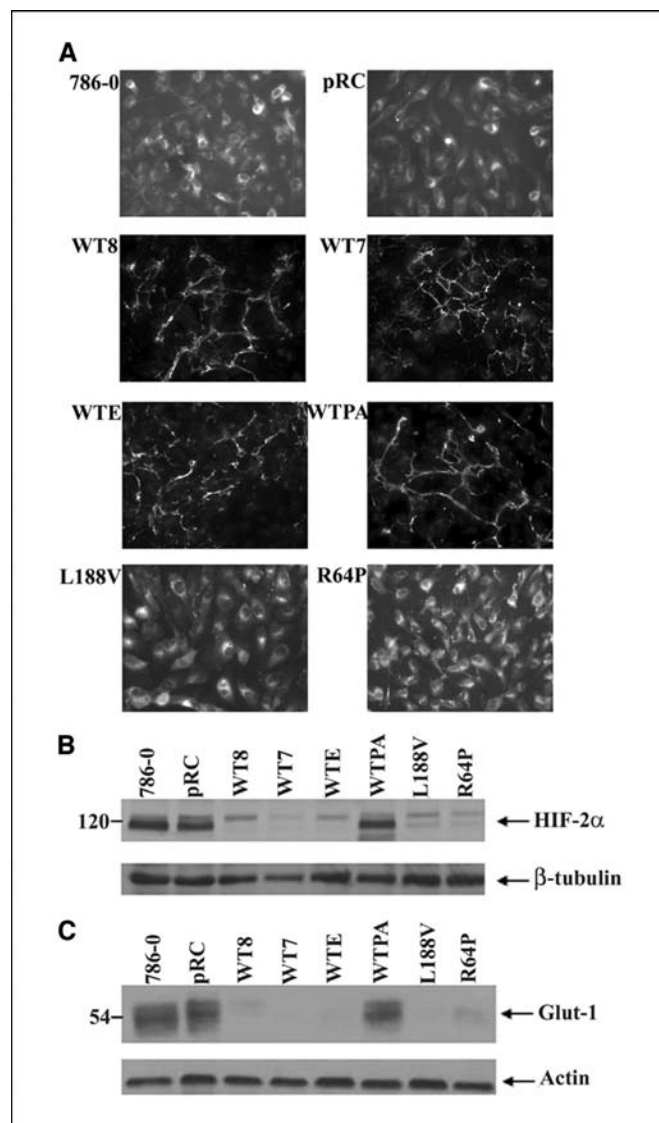


Figure 1. Detection of fibronectin matrix assembly using indirect immunofluorescence. *A*, the various cell lines were grown on coverslips for 6 days. Fibronectin matrix assembly was verified by indirect immunofluorescence, using a monoclonal antifibronectin antibody. Cells expressing wild-type VHL (WT8, WT7, WTE, and WTPA) were able to assemble a distinguishable fibronectin matrix, in contrast to VHL-defective cells (786-0, pRC, L188V, and R64P). This phenomenon is regulated by VHL in a HIF-2 α -independent manner (magnification, $\times 40$). *B*, HIF-2 α expression. Using an anti HIF-2 α polyclonal antibody, HIF-2 α levels were found to be elevated in cells lacking VHL (786-0 and pRC; lanes 1 and 2) as well as in WTPA cells which express a nondegradable form of HIF-2 α (lane 6). This is in contrast to the low levels detected in WT8, WT7, and WTE cells (lanes 3, 4, and 5). Cells harboring type 2C VHL mutants, L188V and R64P, maintain the ability to degrade HIF-2 α , resulting in barely detectable HIF-2 α levels (lanes 7 and 8). Tubulin was used as a loading control. *C*, functionality of HIF-2 α was assessed by verifying the expression levels of its target gene GLUT-1 using a polyclonal anti-GLUT-1 antibody. All cells overexpressing HIF-2 α showed increased levels of GLUT-1. Actin was used as a loading control.

(pH 8.0), 120 mmol/L NaCl, 0.5% NP40] supplemented with protease inhibitors. They were then boiled in SDS-containing sample buffer prior to loading on SDS-PAGE gels. For the fibronectin and collagen IV secretion experiments, the cells were grown in DMEM + 0.1% BSA for 35 hours. The medium was then collected and concentrated using Amicon centrifugal filters devices (Millipore, Nepean, Ontario, Canada). The samples were normalized to intracellular protein concentration then boiled in SDS-containing sample buffer and loaded on SDS-PAGE gels.

Invasion and zymogram assays. Polycarbonate inserts (8 μ m pore, Fisher, Nepean, Ontario, Canada) were first coated with growth factor-reduced (GFR) Matrigel (BD Biosciences) diluted in serum-free DMEM. Cells (10^4) in complete medium (DMEM + 10% FBS) were then plated on the Matrigel layer and allowed to invade for 22 hours. They were then fixed with 10% neutral buffered formalin (Surgipath Canada, Inc., Winnipeg, Manitoba, Canada) and stained with 0.1% crystal violet solution (Sigma). The Matrigel layer was scraped off with a cotton swab followed by visualization using a light microscope. The experiments were repeated in triplicate and cell counts were based on four different fields per experiment.

Zymogram assays were done using conditioned medium from the various cell lines. Cells were grown in 0.1% BSA for 35 hours and the media was then collected and concentrated using Amicon centrifugal filters devices. The samples were normalized for intracellular protein concentration followed by PAGE on 0.1% gelatin gels. The gels were then washed in a solution of 2.5% Triton in 10 mmol/L Tris-HCl (pH 7.5) for 1 hour followed by a 15-minute wash with 10 mmol/L Tris-HCl (pH 8.0). They were then incubated in a zymogram buffer containing 50 mmol/L Tris-HCl (pH 8.0), and 10 mmol/L CaCl₂ overnight at 37°C. Gelatinolytic activity was then observed by staining with 0.5% Coomassie blue.

Statistical analysis. Student's *t* test was used to analyze the differences in terms of mean tumor volume, microvessel density, and VEGF protein levels. Statistical significance was accepted for a value of $P < 0.05$.

Results

Derivatives of the 786-0 RCC cell line provide a system to study the VHL pathways involved in suppression of tumorigenesis and angiogenesis. VHL operates along two pathways, the first leading to HIF- α degradation and the second resulting in ECM assembly. The role of VHL in suppressing tumor formation through HIF-2 α regulation has been established, but it is not clear how loss of ECM assembly leads to tumor formation. We used the VHL-negative RCC cell line 786-0 and its derivatives to dissect and study these two pathways separately. 786-0 cells only express the HIF-2 α isoform. We tested these RCC cell lines for their ability to assemble an ECM matrix and we observed that cells lacking VHL function failed to assemble a fibronectin matrix (Fig. 1A), whereas reintroduction of VHL restored fibronectin assembly as shown previously (17). To determine whether disruption of the VHL-HIF-2 α degradation pathway abolishes fibronectin matrix assembly, we used WTPA cells which are VHL-positive (VHL+) cells retrovirally infected to produce a nondegradable form of HIF-2 α . WTE cells, which are VHL+ cells infected with an empty virus, were used as control for WTPA cells (25). Our results showed that WTPA cells can assemble a fibronectin matrix similar to the VHL+ cells (Fig. 1A). Therefore, disruption of the VHL-HIF-2 α degradation pathway does not affect the ability of RCC cells expressing WT-VHL to regulate ECM assembly. WTPA cells provide a system whereby only the VHL-HIF-2 α degradation pathway is disrupted but the VHL-ECM assembly pathway is still functional. Cells expressing type 2C VHL mutants, L188V and R64P, failed to assemble a fibronectin matrix as described previously (18, 19). These VHL mutant-expressing cells provide an important tool to individually study the effect of loss of the VHL-ECM assembly pathway. The presence of HIF-2 α

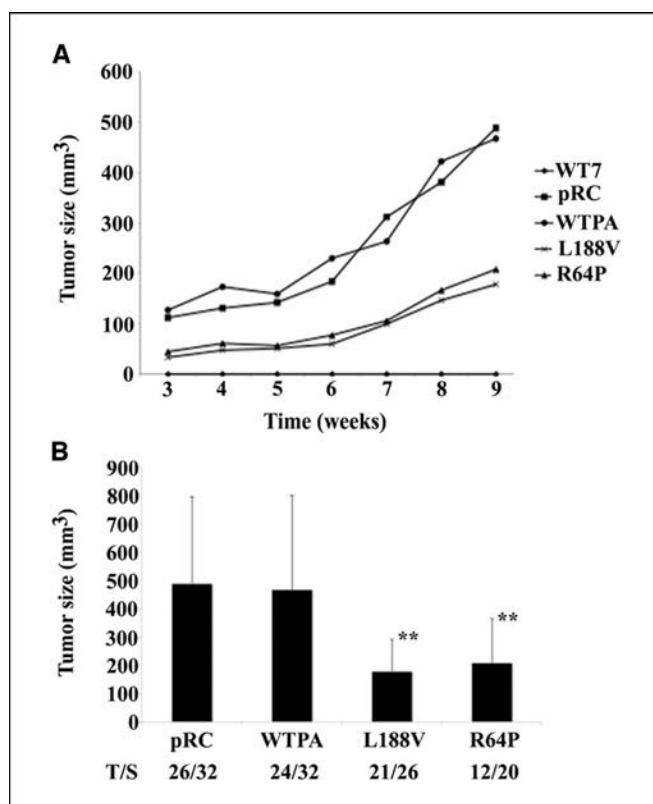


Figure 2. Tumorigenic potential of the various cell lines. Nude mice were injected s.c. with the various cell lines. Tumors were measured with calipers weekly and tumor volume (mm³) was calculated. *A*, growth curves of xenografts showing the mean tumor volume. All the cell lines formed tumors with the exception of WT7. *B*, mean tumor volumes 9 weeks after the s.c. implantation of the cells; bars, SD. T/S, number of tumors formed / number of sites injected. **, $P < 0.01$ versus pRC group.

was assessed in the different cell lines by Western blot (Fig. 1B) and its functionality was determined by the expression of one of its target genes, GLUT-1 (Fig. 1C).

Inactivation of the VHL-ECM assembly pathway is involved in tumor formation. It was reported that loss of ECM integrity influences cellular transformation and tumorigenesis *in vivo* (26). Therefore, we examined whether inactivation of the VHL-ECM assembly pathway contributes to tumorigenesis. To this end, we injected the various RCC cell lines s.c. into the flanks of nude mice. Nine weeks after the inoculation, tumor formation was observed with cells that have lost the VHL-HIF-2 α degradation pathway (WTPA) as well as with cells that have lost regulation of both VHL-ECM assembly and VHL-HIF-2 α degradation pathways (pRC) as previously described (Fig. 2A; ref. 25). In contrast, cells expressing wild-type VHL (WT7) failed to form tumors. Interestingly, the cell lines defective in the VHL-ECM assembly pathway (L188V and R64P) also formed tumors that developed with a later onset than tumors derived from pRC and WTPA cells with the tumor incidence comparable for all cell types (Fig. 2A and B). These results suggest that VHL suppresses tumor formation by operating along both pathways: ECM assembly and HIF-2 α degradation. Our data, using naturally occurring VHL mutants, substantiate the findings of Stickle et al. In their report, a VHL mutant defective for neddylation, which failed to assemble a fibronectin matrix but could still degrade HIF- α , lead to tumor formation (23).

Highly angiogenic tumors result from loss of the VHL-ECM assembly pathway and not the VHL-HIF-2 α degradation pathway. VHL disease is characterized by the formation of highly vascularized tumors. In order to identify which pathway is responsible for angiogenesis in this RCC model, we examined blood vessel formation by staining the different tumors for an endothelial cell marker, CD31 (Fig. 3A). As previously observed, pRC cells, lacking both the VHL-HIF-2 α degradation and VHL-ECM assembly pathways, formed highly vascularized tumors as compared with the ones formed by the cells lacking only the VHL-HIF-2 α degradation pathway (WTPA; ref. 25). Very interestingly, tumors derived from cell lines lacking a functional VHL-ECM assembly pathway (L188V and R64P) were highly vascularized similar to tumors obtained with pRC cells (Fig. 3A). The differences in vascularization were confirmed by quantification of the microvessel density for each type of tumor (Fig. 3B). A three times more significant decrease was observed in the microvessel density of the WTPA tumors as compared with the other types of tumors ($P < 0.01$ versus pRC; $P < 0.001$ versus L188V and R64P). Poor vascularization and low microvessel density comparable to the WTPA tumors were also observed in other RCC tumors derived from cells expressing wild-type VHL, SKRC-39 (data not shown). Necrotic areas which were mainly detected in WTPA tumors were probably due to lack of vascularization (Fig. 3A, arrow). These results suggest that the development of a vascular network following pVHL inactivation

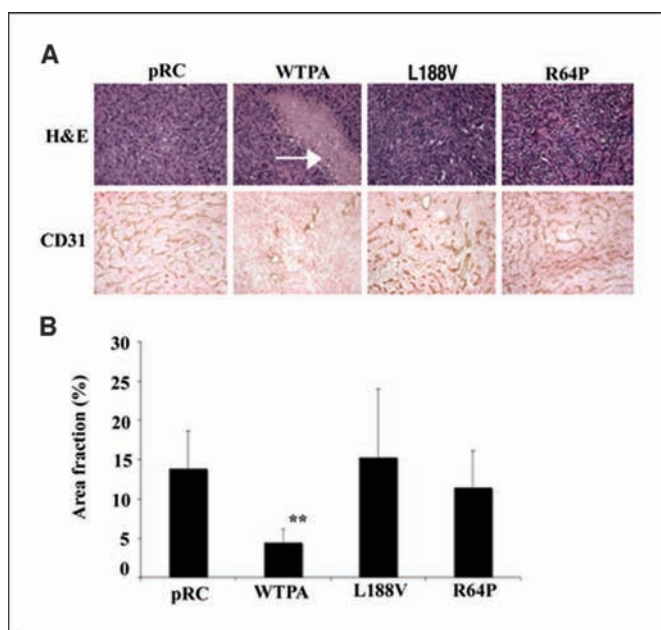


Figure 3. Determination of the VHL pathway involved in angiogenesis. *A*, representative histologic sections stained with H&E for common tumor histology. Note that WTPA tumors present areas of necrosis (arrow) in contrast to the tumors defective for the VHL-ECM assembly pathway. To analyze the vascularization of the various tumors, frozen sections were stained with an antibody against CD31. pRC cells, defective in both the VHL-HIF-2 α degradation and VHL-ECM assembly pathways, as well as L188V and R64P cells, which are defective only in the VHL-ECM assembly pathway showed increased CD31 staining as compared with WTPA tumors defective in the VHL-HIF-2 α degradation pathway only. *B*, quantification of CD31 levels was done blindly and is presented in terms of area fraction occupied by the microvessels per microscope field (expressed as a percentage). WTPA tumors ($4.5 \pm 1.7\%$), defective in the HIF-2 α pathway, displayed significantly fewer microvessels as compared with the other three cell types, pRC ($13.9 \pm 4.8\%$), L188V ($15.5 \pm 8.6\%$), and R64P ($11.5 \pm 4.7\%$). **, $P < 0.01$ versus pRC group (magnification, $\times 20$).

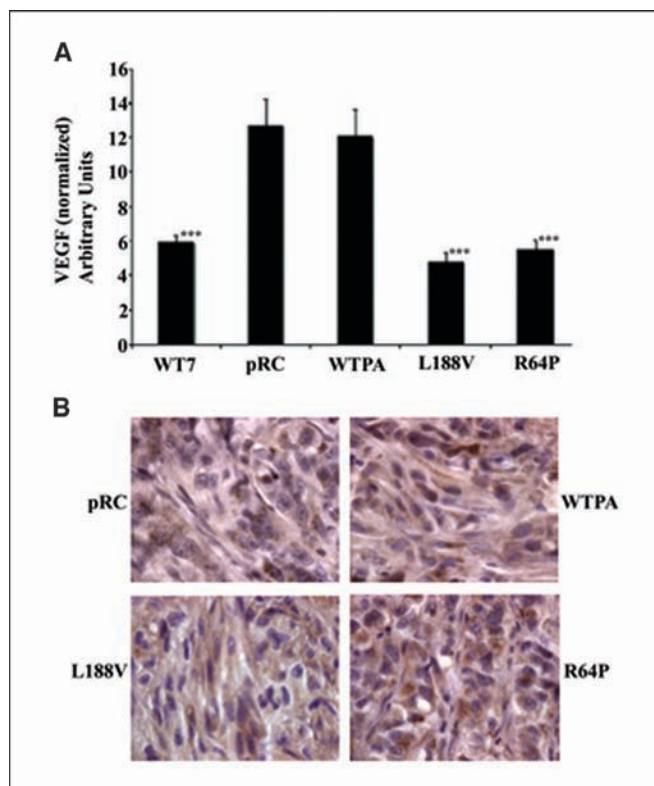


Figure 4. Expression of VEGF protein in cells and tumors. *A*, $\sim 5 \times 10^4$ cells of the various cell lines were plated on six-well plates and allowed to grow in normal growth medium. Conditioned supernatant was harvested after 72 hours, and VEGF protein levels analyzed by an ELISA assay. VEGF values were normalized to total cellular protein concentration and represent the mean from two independent experiments. VEGF protein levels are elevated in pRC (12.7 ± 1.6) and WTPA (12.1 ± 1.6) cell lines as compared with WT7 (5.9 ± 0.3), L188V (4.8 ± 0.6) and R64P (5.5 ± 0.6). ***, $P < 0.001$ versus pRC group. *B*, histochemical analysis of VEGF expression in the various tumors. All tumors showed comparable VEGF staining (magnification, $\times 100$).

occurs upon loss of the VHL-ECM assembly pathway and is not only dependent on the VHL-HIF-2 α degradation pathway.

Expression and secretion of VEGF is not sufficient to develop a vascular network in RCC tumors. Tumors secrete a variety of angiogenic factors including VEGF. To examine if the high level of angiogenesis observed with the VHL tumors was due to an increase in VEGF levels, we first measured secreted VEGF protein levels in the different cell lines using an ELISA assay. Due to the induction of VEGF expression by increased HIF-2 α levels, WTPA, as well as pRC cell lines had a significant 2-fold increase in secreted VEGF levels over cell lines expressing wild-type VHL (WT7) and those that have lost the VHL-ECM assembly pathway only (L188V and R64P; Fig. 4A). The higher VEGF levels in the pRC and WTPA cells were due to induction of VEGF expression by increased HIF-2 α levels. We then did indirect immunostaining on paraffin sections of the different tumors to verify the VEGF status *in vivo* and observed similar VEGF staining in all tumors (Fig. 4B). We also investigated the expression of the different VEGF isoforms in tumors using semiquantitative reverse transcription-PCR and found that they were expressed equally in tumors (data not shown). These results suggest that, although the increase in VEGF levels upon loss of the VHL-HIF-2 α degradation pathway leads to modest tumor vascularization, loss of the VHL-ECM assembly pathway is responsible for the extensive angiogenic network of VHL tumors.

Tumors formed upon loss of the VHL-ECM assembly pathway display a loosely remodeled ECM. Because VEGF is expressed in all tumors, it was surprising that WTPA tumors were so poorly vascularized as compared with L188V and R64P tumors. It was shown that VEGF can be sequestered by ECM proteins and released upon ECM remodeling by matrix metalloproteinases (MMP; refs. 21, 27). Therefore, we examined ECM deposition within tumors formed by the different cell lines. Because fibronectin and collagen type IV are two major proteins of the ECM, we did immunofluorescence staining of both proteins on frozen sections of the various tumors (Fig. 5A). The fibronectin and collagen type IV matrices within the tumors derived from cell lines that have lost the VHL-ECM assembly pathway (L188V and R64P) and those that have lost both VHL-HIF-2 α degradation and VHL-ECM assembly pathways (pRC) were loose and aberrant as opposed to tumors formed by WTPA cells that have lost the HIF-2 α degradation pathway (Fig. 5A). The latter tumors exhibited a dense and organized fibronectin and collagen type IV network that was evenly distributed throughout the tumor sections. This ECM organization is similar to other RCC tumors derived from the SKRC-39 cell line (wild-type VHL; data not shown). These results suggest that dysregulation of the VHL-ECM assembly pathway, leading to an aberrant ECM, is required for the distribution of blood vessels throughout VHL tumors.

Disorganization of the ECM in VHL tumors does not result from a defect in expression or secretion of ECM proteins. We tested whether there was a defect in expression or secretion of fibronectin and collagen type IV which would explain why VHL mutant cells fail to assemble an ECM. We did Western blot analysis using total cell lysates from the different cell lines. All the cell lines tested, including VHL mutant cell lines, produced fibronectin and collagen type IV (Fig. 5B). The expression levels of fibronectin and collagen type IV varied among the different cell types and showed no correlation with the ability of cells to assemble an ECM. To verify whether there was a defect in secretion of the two proteins in the cells expressing mutant forms of VHL, we did a Western blot analysis of secreted fibronectin and collagen type IV in the cell culture media. Although they were unable to assemble an ECM, VHL-defective cells, similar to cells expressing wild-type VHL, maintained the ability to secrete fibronectin and collagen type IV (Fig. 5C).

Loss of the VHL-ECM assembly pathway results in an invasive behavior of cells. Tumor angiogenesis requires ECM degradation which enables blood vessels to penetrate the basal lamina and invade the tumor tissue. It was shown that cells lacking VHL are invasive whereas reintroduction of VHL suppresses their invasive ability (28). We tested the ability of the different VHL mutant cell lines to invade GFR Matrigel. Our results showed that cells that have lost the VHL-ECM assembly pathway (L188V and R64P), and cells that have lost both the VHL-ECM assembly and VHL-HIF-2 α degradation pathways (786-0 and pRC) were highly invasive (Fig. 6A) and expressed high MMP-2 levels as determined by Western blot analysis (Fig. 6B). The MMP-2 protein levels correlated with MMP-2 activity when tested in zymogram assays (Fig. 6C). Conditioned medium from primary rat smooth muscle cells, which express high levels of MMP-2, were used as a positive control (data not shown). Reintroduction of wild-type VHL in WT8, WT7, and WTE cells suppressed their invasive capacity by at least 4-fold. Cells that have only lost the VHL-HIF-2 α degradation pathway (WTPA

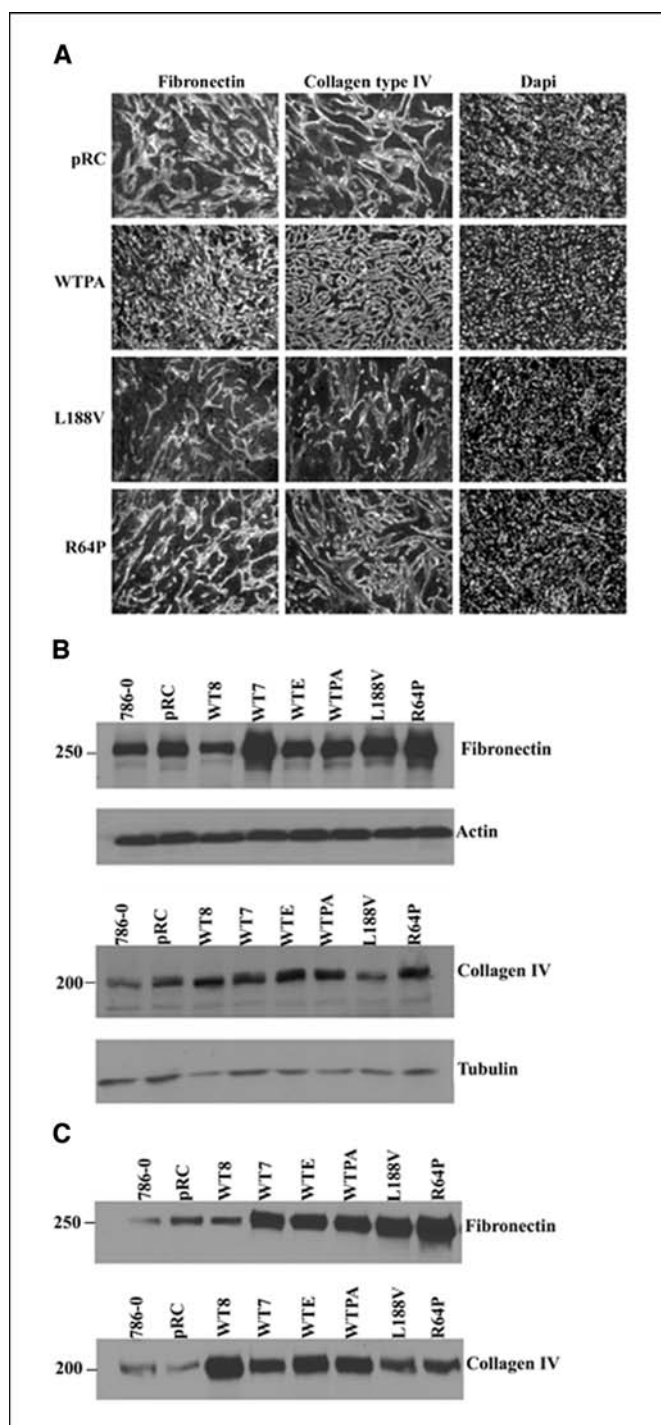


Figure 5. Analysis of ECM proteins in tumors and cells. *A*, tumor sections were stained for the ECM proteins, fibronectin and collagen type IV. WTPA cells, defective for the VHL-HIF-2 α degradation pathway, displayed a dense and tightly organized network of fibronectin and collagen type IV. In contrast, pRC cells, lacking both the VHL-HIF-2 α degradation and VHL-ECM assembly pathways, as well as L188V and R64P cells, which are defective only in the VHL-ECM assembly pathway, displayed a loose network of both ECM proteins (magnification, $\times 20$). *B*, fibronectin and collagen IV expression. Cells were lysed using EBC buffer and total lysates were loaded on SDS-6% PAGE gels. All cells expressed significant levels of fibronectin and collagen IV regardless of their VHL status. Actin and tubulin were used as loading controls. *C*, fibronectin and collagen type IV secretion. Cells were grown in DMEM 0.1% BSA for 35 hours, the medium was then collected and concentrated, and then loaded on SDS-6% PAGE gels. All cells secreted fibronectin and collagen IV with variable patterns regardless of their VHL status.

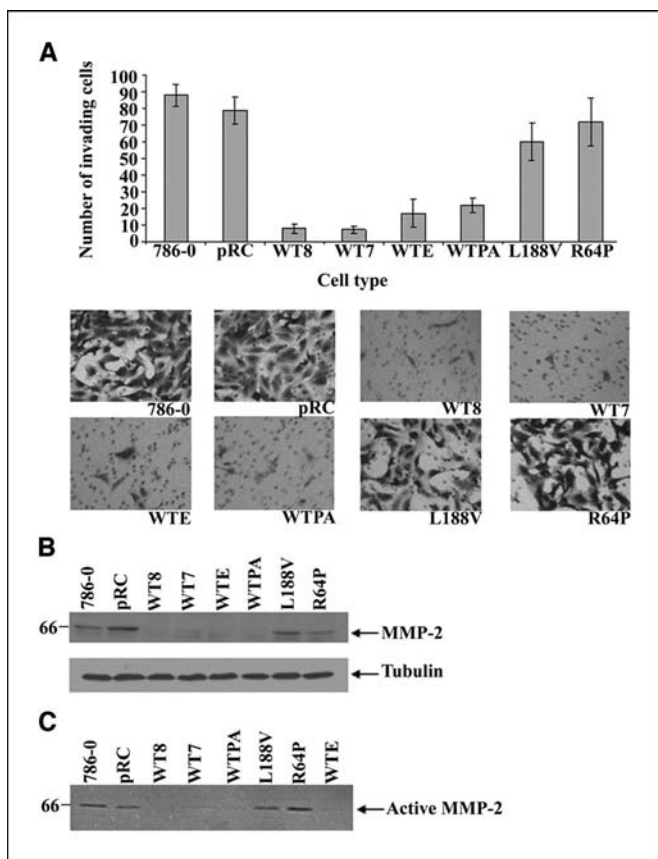


Figure 6. Ability of the different cell lines to invade through GFR Matrigel. **A**, Matrigel invasion assay. The different cell lines were incubated on GFR Matrigels for 22 hours. The cells were then fixed and stained and the extent of invasion determined for each cell type. Cell lines lacking the VHL-ECM assembly pathway (L188V and R64P) showed increased invasive capacity similar to cell lines that are defective for both VHL-ECM assembly and VHL-HIF-2 α degradation pathways (786-0 and pRC). Invasiveness is suppressed by at least 4-fold through the reintroduction of wild-type VHL (WT8, WT7, and WTE). Cells that have lost the VHL-HIF-2 α degradation pathway (WTPA) did not show any marked increase in invasive ability. **B**, MMP expression. The cells that were found to be invasive in Matrigel exhibited increased MMP-2 levels as compared with the cells with low invasive ability. **C**, increased MMP-2 levels correlate with MMP-2 activity in gelatin gels.

cells) were significantly less invasive with diminished MMP-2 expression and activity, suggesting that loss of the HIF-2 α degradation pathway does not promote invasiveness in this RCC setting (Fig. 6A and B). These data suggest that loss of the VHL-ECM assembly pathway leads to an increase in cell invasion and ECM degradation resulting in an aberrant tumor matrix and promotion of tumor angiogenesis.

Discussion

VHL inactivation leads to the development of tumors densely infiltrated with blood vessels. VHL functions along two pathways: the first leading to tumor suppression by HIF-2 α degradation, and the second involving ECM regulation. HIF-2 α controls many cellular processes including stimulation of VEGF expression which leads to increased angiogenesis (16, 29, 30), and induction of serum-independent cell proliferation (31). The high level of vascularization of VHL tumors has been attributed to VEGF overexpression. By binding to its receptors, VEGF could trigger an angiogenic response by acting on the proliferation, migration, and

survival of endothelial cells (32). However, it has been reported that tumor vascularization upon VHL loss is a result of more than just HIF- α up-regulation (25). Other reports showed that the loss of HIF-1 α negatively affects tumorigenesis (16, 33) and reduction in tumor growth was not due to a decrease in vascularization (33).

Because the function of the VHL-ECM assembly pathway is poorly understood, we verified its role in suppression of tumorigenesis and angiogenesis using a cell system where the two pathways (VHL-HIF-2 α degradation and VHL-ECM assembly) were uncoupled. Loss of the VHL-ECM assembly pathway led to the formation of tumors. This is in contrast to a study by Hoffman et al. (18) where L188V cells did not form tumors. This discrepancy could be due to a shorter incubation time in nude mice. However, our data are in accordance with Stickle et al., who used a VHL mutant defective for fibronectin matrix assembly (23). In addition, tumors observed upon loss of the VHL-ECM assembly pathway (L188V and R64P) were highly angiogenic and such important vascularization was not observed in tumors overexpressing HIF-2 α , although they secreted 2-fold more VEGF *in vitro*. These latter tumors grew quickly, suggesting that loss of the VHL-HIF-2 α degradation pathway is required for mediating the growth of VHL tumors probably due to overexpression of transforming growth factor- α and cyclin D1 (16). On the other hand, loss of the VHL-ECM assembly pathway seems to be required for full-scale tumor angiogenesis in this RCC setting.

Loss of the VHL-HIF-2 α degradation pathway does not disrupt the fibronectin and collagen type IV network whereas loss of the VHL-ECM assembly pathway leads to an aberrant ECM assembly and stimulation of angiogenesis. Remodeling of the ECM during tumor angiogenesis is triggered by secreted proteases such as MMPs (34) and these were found to play an important role in angiogenesis. MMPs could increase the release and activation of matrix-sequestered angiogenic factors, such as VEGF (21, 27). VEGF has been documented to be an important inducer of tumor angiogenesis and a 2-fold increase in its expression level was shown to cause an angiogenic response using an *in vitro* angiogenesis assay (20). Therefore, it is possible that in VHL tumors lacking the VHL-HIF-2 α degradation pathway, the intact ECM serves to sequester the secreted VEGF thus hindering it from stimulating proliferation and migration of endothelial cells (WTPA tumors). Remodeling of the ECM by MMP-2, which is activated upon loss of the VHL-ECM assembly pathway, might result in the release of VEGF to exert its angiogenic effect.

As a result of their remodeling activities, MMPs were shown to expose cryptic sites within collagen type IV and this is associated with a gain of binding to $\alpha v \beta 3$ integrin on endothelial cells and stimulation of angiogenesis (35, 36). Disruption of MMP-2 binding to $\alpha v \beta 3$ was shown to inhibit tumor growth and vascularization *in vivo* (37). Moreover, it was shown that angiogenesis and tumor growth are suppressed in MMP-2 knockout mice (38). Therefore, it is possible that in tumors which have lost the VHL-ECM assembly pathway, remodeling of the ECM by MMP-2 allows exposure of cryptic sites within ECM proteins which could stimulate tumor growth and angiogenesis.

In conclusion, we propose that loss of the VHL-ECM assembly pathway could have several consequences: (a) removal of a barrier to facilitate growth and invasion of blood vessels, (b) release of ECM sequestered factors such as VEGF, (c) presentation of cryptic sites on ECM proteins resulting in increased neovascularization. Loss of VHL function drives tumorigenesis and angiogenesis along,

at least, the VHL-HIF-2 α degradation and VHL-ECM assembly pathways. Although HIF-2 α activation leads to VEGF overexpression, our results suggest that progression of the complete tumor angiogenic response is observed on loss of the VHL-ECM assembly pathway resulting in extensive VHL tumor vascularization. These results stress the importance of elucidating the mechanism of the VHL-ECM pathway which seems to be involved in tumorigenesis, angiogenesis, and cell invasion.

Acknowledgments

Received 7/20/2005; revised 11/7/2005; accepted 11/23/2005.

References

- Kaelin WG, Jr. Molecular basis of the VHL hereditary cancer syndrome. *Nat Rev Cancer* 2002;2:673–82.
- Richards FM, Webster AR, McMahon R, Woodward ER, Rose S, Maher ER. Molecular genetic analysis of von Hippel-Lindau disease. *J Intern Med* 1998;243:527–33.
- Kondo K, Kaelin WG, Jr. The von Hippel-Lindau tumor suppressor gene. *Exp Cell Res* 2001;264:117–25.
- Richard S, Campello C, Taillandier L, Parker F, Resche F. Haemangioblastoma of the central nervous system in von Hippel-Lindau disease. French VHL Study Group. *J Intern Med* 1998;243:547–53.
- Folkman J. Tumor angiogenesis: therapeutic implications. *N Engl J Med* 1971;285:1182–6.
- Folkman J. Angiogenesis in cancer, vascular, rheumatoid and other disease. *Nat Med* 1995;1:27–31.
- Hanahan D, Folkman J. Patterns and emerging mechanisms of the angiogenic switch during tumorigenesis. *Cell* 1996;86:353–64.
- Safran M, Kaelin WG, Jr. HIF hydroxylation and the mammalian oxygen-sensing pathway. *J Clin Invest* 2003; 111:779–83.
- Iwai K, Yamanaka K, Kamura T, et al. Identification of the von Hippel-Lindau tumor-suppressor protein as part of an active E3 ubiquitin ligase complex. *Proc Natl Acad Sci U S A* 1999;96:12436–41.
- Ohh M, Park CW, Ivan M, et al. Ubiquitination of hypoxia-inducible factor requires direct binding to the β -domain of the von Hippel-Lindau protein. *Nat Cell Biol* 2000;2:423–7.
- Maxwell PH, Wiesener MS, Chang GW, et al. The tumour suppressor protein VHL targets hypoxia-inducible factors for oxygen-dependent proteolysis. *Nature* 1999;399:271–5.
- Ivan M, Kondo K, Yang H, et al. HIF- α targeted for VHL-mediated destruction by proline hydroxylation: implications for O₂ sensing. *Science* 2001;292:464–8.
- Jaakkola P, Mole DR, Tian YM, et al. Targeting of HIF- α to the von Hippel-Lindau ubiquitylation complex by O₂-regulated prolyl hydroxylation. *Science* 2001;292:468–72.
- Epstein AC, Gleadle JM, McNeill LA, et al. *C. elegans* EGL-9 and mammalian homologs define a family of dioxygenases that regulate HIF by prolyl hydroxylation. *Cell* 2001;107:43–54.
- Bruick RK, McKnight SL. A conserved family of prolyl-4-hydroxylases that modify HIF. *Science* 2001;294: 1337–40.
- Raval RR, Lau KW, Tran MG, et al. Contrasting properties of hypoxia-inducible factor 1 (HIF-1) and HIF-2 in von Hippel-Lindau-associated renal cell carcinoma. *Mol Cell Biol* 2005;25:5675–86.
- Ohh M, Yauch RL, Lonergan KM, et al. The von Hippel-Lindau tumor suppressor protein is required for proper assembly of an extracellular fibronectin matrix. *Mol Cell* 1998;1:959–68.
- Hoffman MA, Ohh M, Yang H, Klco JM, Ivan M, Kaelin WG, Jr. von Hippel-Lindau protein mutants linked to type 2C VHL disease preserve the ability to downregulate HIF. *Hum Mol Genet* 2001;10:1019–27.
- Clifford SC, Cockman ME, Smallwood AC, et al. Contrasting effects on HIF-1 α regulation by disease-causing pVHL mutations correlate with patterns of tumorigenesis in von Hippel-Lindau disease. *Hum Mol Genet* 2001;10:1029–38.
- Bergers G, Benjamin LE. Tumorigenesis and the angiogenic switch. *Nat Rev Cancer* 2003;3:401–10.
- Bergers G, Brekken R, McMahon G, et al. Matrix metalloproteinase-9 triggers the angiogenic switch during carcinogenesis. *Nat Cell Biol* 2000;2:737–44.
- Pause A, Lee S, Worrell RA, et al. The von Hippel-Lindau tumor-suppressor gene product forms a stable complex with human CUL-2, a member of the Cdc53 family of proteins. *Proc Natl Acad Sci U S A* 1997;94: 2156–61.
- Stickler NH, Chung J, Klco JM, Hill RP, Kaelin WG, Jr., Ohh M. pVHL modification by NEDD8 is required for fibronectin matrix assembly and suppression of tumor development. *Mol Cell Biol* 2004;24:3251–61.
- Bishop T, Lau KW, Epstein AC, et al. Genetic analysis of pathways regulated by the von Hippel-Lindau tumor suppressor in *Caenorhabditis elegans*. *PLoS Biol* 2004;2: 1549–60.
- Kondo K, Klco J, Nakamura E, Lechpammer M, Kaelin WG, Jr. Inhibition of HIF is necessary for tumor suppression by the von Hippel-Lindau protein. *Cancer Cell* 2002;1:237–46.
- Colombi M, Zoppi N, De Petro G, et al. Matrix assembly induction and cell migration and invasion inhibition by a 13-amino acid fibronectin peptide. *J Biol Chem* 2003;278:14346–55.
- Belotti D, Paganoni P, Manenti L, et al. Matrix metalloproteinases (MMP9 and MMP2) induce the release of vascular endothelial growth factor (VEGF) by ovarian carcinoma cells: implications for ascites formation. *Cancer Res* 2003;63:5224–9.
- Koochekpour S, Jeffers M, Wang PH, et al. The von Hippel-Lindau tumor suppressor gene inhibits hepatocyte growth factor/scatter factor-induced invasion and branching morphogenesis in renal carcinoma cells. *Mol Cell Biol* 1999;19:5902–12.
- Maxwell PH, Ratcliffe PJ. Oxygen sensors and angiogenesis. *Semin Cell Dev Biol* 2002;13:29–37.
- Clifford SC, Maher ER. von Hippel-Lindau disease: clinical and molecular perspectives. *Adv Cancer Res* 2001;82:85–105.
- Gunaratnam L, Morley M, Franovic A, et al. Hypoxia inducible factor activates the transforming growth factor- α /epidermal growth factor receptor growth stimulatory pathway in VHL(-/-) renal cell carcinoma cells. *J Biol Chem* 2003;278:44966–74.
- Ferrara N, Carver-Moore K, Chen H, et al. Vascular endothelial growth factor: basic science and clinical progress. *Endocr Rev* 2004;25:581–611.
- Ryan HE, Poloni M, McNulty W, et al. Hypoxia-inducible factor-1 α is a positive factor in solid tumor growth. *Cancer Res* 2000;60:4010–5.
- Handsley MM, Edwards DR. Metalloproteinases and their inhibitors in tumor angiogenesis. *Int J Cancer* 2005; 115:849–60.
- Xu J, Rodriguez D, Petitsclerc E, et al. Proteolytic exposure of a cryptic site within collagen type IV is required for angiogenesis and tumor growth *in vivo*. *J Cell Biol* 2001;154:1069–79.
- Hangai M, Kitaya N, Xu J, et al. Matrix metalloproteinase-9-dependent exposure of a cryptic migratory control site in collagen is required before retinal angiogenesis. *Am J Pathol* 2002;161:1429–37.
- Silletti S, Kessler T, Goldberg J, Boger DL, Cheresh DA. Disruption of matrix metalloproteinase 2 binding to integrin $\alpha v \beta 3$ by an organic molecule inhibits angiogenesis and tumor growth *in vivo*. *Proc Natl Acad Sci U S A* 2001;98:119–24.
- Itoh T, Tanioka M, Yoshida H, Yoshioka T, Nishimoto H, Itohara S. Reduced angiogenesis and tumor progression in gelatinase A-deficient mice. *Cancer Res* 1998;58: 1048–51.